

# Shortening X-ray Pulses for Pump-Probe Experiments at Synchrotrons

H. Navirian,<sup>1</sup> M. Herzog,<sup>2, a)</sup> Y. Goldshteyn,<sup>1</sup> W. Leitenberger,<sup>2</sup> I. Vrejoiu,<sup>3</sup> D. Khakhulin,<sup>4</sup> M. Wulff,<sup>4</sup> R. Shayduk,<sup>1</sup> P. Gaal,<sup>2</sup> and M. Bargheer<sup>1, 2</sup>

<sup>1)</sup>*Helmholtz-Zentrum Berlin für Materialien und Energie GmbH, Wilhelm-Conrad-Röntgen Campus, BESSY II, Albert-Einstein-Str. 15, 12489 Berlin Germany*

<sup>2)</sup>*Institut für Physik und Astronomie, Universität Potsdam, Karl-Liebknecht-Str. 24-25, 14476 Potsdam, Germany*

<sup>3)</sup>*Max-Planck-Institut für Mikrostrukturphysik, Weinberg 2, 06120 Halle, Germany*

<sup>4)</sup>*European Synchrotron Radiation Facility (ESRF), 6 rue Jules Horowitz 38000 Grenoble, France*

(Dated: 3 February 2011)

We implemented an experimental scheme for ultrafast x-ray diffraction (UXRD) at storage rings based on a laser-driven Bragg-switch that shortens the x-ray pulses emitted from an undulator. The increased time-resolution is demonstrated by observing changes of intensity, position and width of the diffraction peaks of an  $\text{La}_{0.7}\text{Sr}_{0.3}\text{MnO}_3/\text{SrTiO}_3$  superlattice sample after optical excitation, i.e., by quantitatively measuring the propagation of an expansion wave through the sample. These experimental transients with timescales of 35 to 60 ps evidence a reduction of the x-ray pulse duration by a factor of two.

PACS numbers: 61.05.cp, 78.47.J, 61.05.C, 68.65.Cd, 78.70.Ck

Keywords: X-ray diffraction, Ultrafast, Superlattice

Hard x-rays derived from modern synchrotron light sources have ideal properties for structure analysis by x-ray diffraction. The x-rays are generated by short electron bunches traveling in storage rings, yielding x-ray pulses with a duration on the order of 150 ps. Ultrafast x-ray diffraction (UXRD) uses this time structure in order to access the transient dynamics by pump-probe experiments. An optical pump pulse excites atomic motion in a sample and a time-delayed hard x-ray probe pulse measures the lattice changes for different delay times  $\tau$ , creating a series of snapshots of the atomic positions. In this stroboscopic scheme the time-resolution is limited by the x-ray pulse duration. One option to obtain  $\approx 100$  fs x-ray pulses—albeit with relatively low photon flux—is slicing of the electron bunches in an undulator using intense femtosecond laser pulses.<sup>1-3</sup> Because this well-established method is operational at only few beamlines worldwide, and the x-ray free electron lasers (XFELs) will add only few experimental stations<sup>4</sup>, alternative methods are explored. The “low alpha mode” shortens synchrotron pulses considerably, but simultaneously reduces the x-ray flux at all beamlines around the same storage ring.<sup>5,6</sup> Finally, laser-driven X-ray plasma sources have the advantage of being a table-top setup, but lack the flexible tunability of wavelength.<sup>7</sup> The nearly instantaneous drop of the Debye-Waller factor in laser excited InSb was exploited to shorten x-ray pulses, however, this method has not been implemented into a long term stable setup.<sup>8</sup> Recently, we have demonstrated the potential of using coherent phonons in superlattices (SL) to realize switchable Bragg mirrors, which can reduce the pulse duration down to 1 ps.<sup>9</sup>

In this letter, we report on the implementation of this scheme at a synchrotron beamline, however, we exploit the somewhat slower change of the Bragg-peak position to truncate the x-ray pulse, instead of the structure-factor change discussed previously which leads to a se-

ries of ultrashort x-ray bursts.<sup>9</sup> The modified x-rays diffracted from a  $\text{SrRuO}_3/\text{SrTiO}_3$  (SRO/STO) SL are subsequently used as a probe for the transient x-ray response of a  $\text{La}_{0.7}\text{Sr}_{0.3}\text{MnO}_3/\text{SrTiO}_3$  (LSMO/STO) SL sample. We demonstrate the shortening of x-ray pulses at the European Synchrotron Radiation Facility (ESRF) by approximately a factor of two down to  $\approx 60$  ps and we were able to record transients with time scales of 35 ps.

The measurements were performed at the undulator beamline ID09B at the ESRF, Grenoble, France. The U20 undulator gap at the beamline was set to obtain hard x-rays around 12 keV which were monochromatized using a cryogenically cooled double Si (111) crystal monochromator and collimated by a water-cooled toroidal mirror. The x-ray beam size was set to  $0.10 \times 0.05$  mm<sup>2</sup> using horizontal and vertical slits. The storage ring was operating in the 4-bunch mode with a current of 10 mA per bunch and 708 ns time separation between them. Fig. 1 shows a schematic of the setup. A Ti:Sapphire laser with an average output power of 4 W at 800 nm wavelength, a repetition rate of  $\approx 1$  kHz and a pulse duration of 600 fs was electronically synchronized with the electron-bunch pattern, allowing for a tunable delay  $\tau_1$  between laser and x-ray pulses. The timing jitter was on the order of 5 ps, much shorter than the x-ray pulse duration. The laser output was split into two parts, one of which was focused onto a  $1.5 \times 1$  mm<sup>2</sup> spot (fluence of 45 mJ/cm<sup>2</sup>) on the Bragg-Switch (BS) being the SRO/STO SL described previously.<sup>9</sup> The second part of the laser was guided onto a  $1.9 \times 1.9$  mm<sup>2</sup> spot (fluence of 2.4 mJ/cm<sup>2</sup>) on a LSMO/STO SL acting as the sample of interest. This epitaxial heterostructure consists of 15 periods of 13.7 nm thick STO layers and 8.8 nm thick layers of the ferromagnetic metal LSMO grown on a 1 mm STO substrate by pulsed laser deposition<sup>10</sup> as determined from high-resolution XRD. The BS and the sample were mounted on independent goniometers enabling *xyz*-positioning and adjustment of the Bragg angles (Fig. 1). A mechanical delay line was used to control the relative timing of the pump pulses for the BS and the

<sup>a)</sup>Electronic mail: marc.herzog@uni-potsdam.de

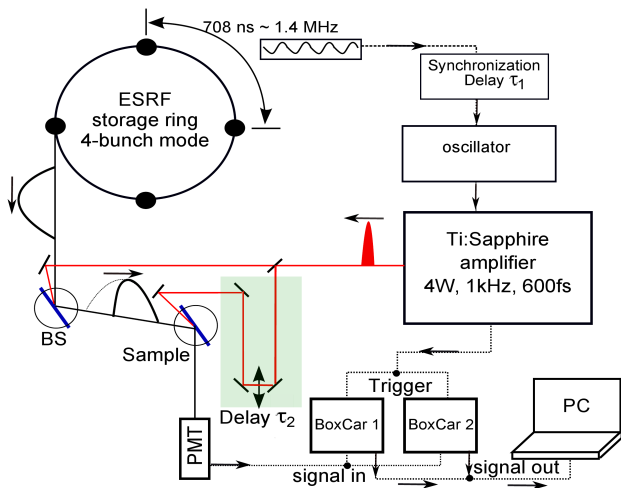


FIG. 1. (Color online) Schematic of the experimental setup. The electronic delay  $\tau_1$  gives the relative timing of the first laser pulse and the x-ray pulse at the Bragg switch (BS). The mechanical delay  $\tau_2$  sets the timing of the excitation of the sample relative to the x-ray pulse emitted by the BS. Next to the x-ray path, we schematically show the temporal profile of the x-ray pulse as it is emitted from the undulator and after truncation by the BS.

sample. Since  $\tau_1$  was set such that the first laser pulse and the ESRF x-ray pulse were coincident at the BS, the delay line effectively varied the time delay  $\tau_2$  between the second laser pulse and the diffracted x-ray pulse at the sample.

The x-ray pulses from the storage ring impinge on the BS at a repetition rate of 1.41 MHz and at a fixed angle  $\Theta_1$  defined by the maximum of the (002) zero-order SL peak (ZOP) and are then diffracted towards the sample.<sup>9,11</sup> These pulses are subsequently diffracted from the sample and detected by a plastic scintillator with a rise-time of 1 ns and a Hamamatsu photomultiplier tube (PMT). The analog output of the PMT is electronically gated by two Boxcar integrators. The first Boxcar is set to detect the x-ray pulses coinciding with a laser pulse (pumped channel) and the second Boxcar monitors the x-ray pulse emitted by the same electron bunch at the preceding round trip (unpumped channel), i.e.  $4 \times 708$  ns earlier (cf. Fig. 1). This way, we are able to evaluate the difference in x-ray reflectivity of the pumped and unpumped sample, respectively, which significantly enhances the signal-to-noise ratio.

In the first part of the experiment, the x-rays diffracted from the BS directly shine on the PMT without reflection from the sample. Delay  $\tau_1$  was varied to record the transient response of the ZOP peak of the BS [red squares in Fig. 2(a)]. The decreasing signal was fitted using the formula

$$\frac{\Delta R(t)}{R_0} = \frac{A}{2} \left[ 1 - \operatorname{erf} \left\{ \frac{4 \ln 2 (\tau - \tau_0)}{\sigma} \right\} \right] \quad (1)$$

where  $A$ ,  $\tau_0$  and  $\sigma$  are the fitting parameters. Here,  $\sigma$  represents the FWHM of the Gaussian corresponding to the derivative of eq. (1) which is also indicated in Figs. 2(b) and (c). The best fit to the data [blue line in Fig. 2(a)] yields  $\sigma = 108.5$  ps which is comparable to but slightly smaller than direct streak camera measurements of the

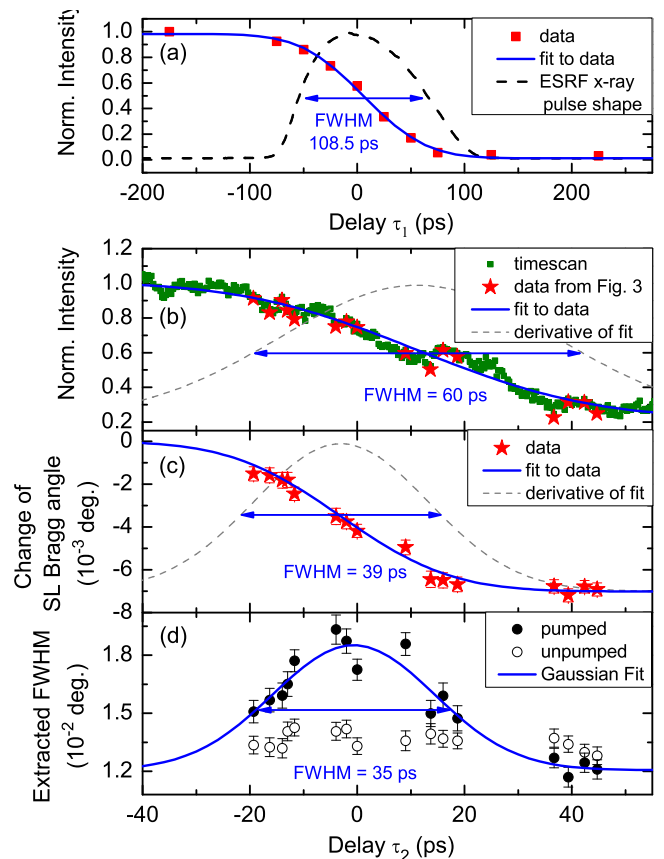


FIG. 2. (Color online) (a) Reflectivity change of BS vs. delay  $\tau_1$  (red squares), fit to the data (solid line) and streak-camera characterization of x-ray pulse shape (dashed line). (b) Reflectivity change of the LSMO/STO ZOP vs. delay  $\tau_2$  from direct measurement (green squares) and derived from rocking curves in Fig. 3 (red stars), fit to the data (solid line) and scaled derivative of the fit (dashed line). The same delay  $\tau_2$  was varied for the next panels: (c) Angular change of the ZOP extracted from Fig. 3 (red stars), fit to the data (solid line) and scaled derivative of the fit (dashed line). (d) Peak width (FWHM) of rocking curves for pumped (bullets) and unpumped sample (circles), and Gaussian fit (solid line).

ESRF x-ray pulse [ $\sigma_{SC} \approx 125$  ps FWHM, dashed line in Fig. 2(a)]. The measured intensity decreases because the Bragg peak position changes to lower angles due to the expansion of the BS triggered by the absorption of the laser pulse.<sup>9,12</sup> The timescale  $T_{\text{shift}}^{\text{BS}} = D_{\text{BS}}/v_{\text{eff}} = 35$  ps for the expansion of the BS is determined by its total thickness ( $D_{\text{BS}} \approx 250$  nm) and its effective sound velocity,  $v_{\text{eff}} \approx 7.2$  nm/ps [ $v_{\text{SRO}} = 6.3$  nm/ps (Ref. 13) and  $v_{\text{STO}} = 7.8$  nm/ps (Ref. 14)].<sup>9,12</sup> The 108.5 ps timescale measured here is obviously limited by the x-ray pulse duration as it is much longer than the intrinsic dynamics of the Bragg peak. If  $\tau_1$  is set to negative values the entire x-ray pulse is reflected from the BS. For large positive  $\tau_1$  the Bragg peak position has changed and the reflectivity of the BS at  $\Theta_1$  reaches a minimum. At intermediate delays the x-ray pulse is only partly reflected and we expect a truncated x-ray pulse as schematically indicated in Fig. 1.

For the second part of the experiment, we set  $\tau_1$  to the value where 60% of the x-ray intensity is reflected and define this as  $\tau_1 = 0$  [cf. Fig. 2(a)]. This time delay

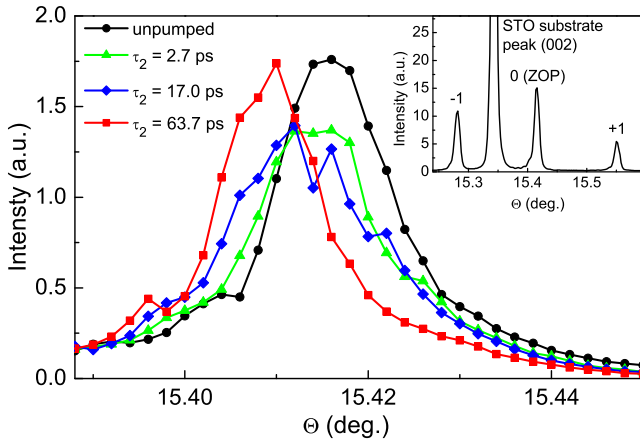


FIG. 3. (Color online) Selected transient rocking curves of the LSMO/STO ZOP used to obtain the data in Fig. 2 (b)-(d). Shown are the scaled unpumped (black bullets) and pumped curves at delays  $\tau_2 = 2.7$  ps (green triangles), 17.0 ps (blue diamonds) and 63.7 ps (red squares). Inset: Extended static rocking curve around STO substrate peak and ZOP.

roughly corresponds to the case where the laser pulse and the maximum of the x-ray pulse coincide. We aligned the LSMO/STO SL sample to be hit by the truncated x-ray pulse and scanned the Bragg angle  $\Theta_2$  of the sample to obtain the extended rocking curve around the (002) STO substrate reflection shown in the inset of Fig. 3. Close to the substrate peak, we identify the ZOP which we will exclusively consider in the following. Fixing the Bragg angle at the maximum of the ZOP and scanning  $\tau_2$ , we recorded the transient presented in Fig. 2(b) which again exhibits a decreasing signal since the expansion of the LSMO/STO SL shifts the Bragg peak to lower angles. The best fit according to eq. (1) yields a FWHM of 60 ps. From the sample thickness  $D_S \approx 340$  nm and the sound velocity of LSMO [ $v_{\text{LSMO}} = 6.5$  nm/ps (Ref. 14)] the timescale of expansion is  $T_{\text{shift}}^S \approx 47$  ps. Both Fig. 2(a) and (b) measure the intensity decrease caused by the shifting SL Bragg peak, and since the ratio of measured and calculated timescale is  $108/35=3.1$  for (a) and  $60/47=1.3$  the x-ray used for measuring the sample must have been approximately a factor of 2 shorter than the 125 ps x-ray pulse of the ESRF, confirming that it was successfully truncated by the BS. Note that shifting  $\tau_1$  to positive (negative) values would truncate the x-ray pulse earlier (later) and would thus diffract shorter (longer) x-ray pulses with an accordingly smaller (larger) total intensity given by Fig. 2(a).

In order to analyze the temporal behavior of the SL Bragg peak of the LSMO/STO sample in more detail, several rocking curves were recorded at fixed pump-probe delays  $\tau_2$ . A selection of these rocking curves is depicted in Fig. 3. The black curve shows the rocking curve recorded with the Boxcar 2, corresponding to the unpumped LSMO/STO SL one synchrotron round trip earlier. This curve has to be scaled down to 60% [cf. Fig. 2(a)] to have approximately the same integrated intensity as those measured with Boxcar 1. The reason is that for these x-ray pulses also the BS is not pumped so that the full non-truncated x-ray pulse hits the sample.

The red curve shows the ZOP of the LSMO/STO SL

at its new position at  $\tau_2 = 63.7$  ps, evidencing a relative expansion of  $\varepsilon = 0.04\%$ . The integrated intensity of the ZOP is constant for all time delays, however, for intermediate times we observe a significant peak broadening as can be directly seen in Fig. 3. In order to quantify the angular change and peak broadening we fitted Gaussian functions to the rocking curves. The extracted peak positions are plotted in Fig. 2(c) as red stars and the FWHM of the Gaussians fits is shown in panel (d). The data show that the change in peak position (FWHM of  $\approx 39$  ps) is accompanied by a transient broadening of the rocking curve (FWHM of  $\approx 35$  ps) which is maximal when the peak position is half-way shifted. Such behavior is expected, since the sound wave which leads to the expansion of the LSMO/STO SL starts from the surface of the SL and propagates towards the substrate.<sup>12</sup> When the expansion front has propagated half way through the SL, we expect a double-peak structure: one peak at the angular position of the unperturbed lattice (black bullets in Fig. 3) from the lower half of the SL and a second peak at the shifted angular position (red squares in Fig. 3) corresponding to the expanded half of the SL close to the surface. In fact, as the separation of these two peaks is relatively small, we measure a broadened rocking curve at intermediate times which also includes interference effects.

In conclusion, we have demonstrated a reliable setup for ultrafast x-ray diffraction (UXRD) at synchrotrons where a laser-driven x-ray Bragg switch is used to significantly decrease and control the pulse duration of hard x-rays by truncation of the initial synchrotron pulse. With these pulses shortened by approximately a factor of two we have performed UXRD experiments on an LSMO/STO superlattice. Not only an expansion by  $\varepsilon = 0.04\%$  could be detected but, moreover, we could reconfirm that the laser excitation in such superlattices transiently broadens the Bragg reflection because at early times the strain propagation yields different lattice constants at the surface and near the substrate. The same setup can be used for switching the pulses down to 1 ps using the principle proposed by Herzog et al.<sup>9</sup>, however, the excitation laser is required to have a pulse duration  $\leq 200$  fs in order to efficiently launch the fast superlattice oscillations.

We thank the BMBF for funding the project via 05K10IP1 and the DFG via SFB 762.

<sup>1</sup>R. Schoenlein, S. Chattopadhyay, H. Chong, T. Glover, P. Heimann, C. Shank, A. Zholents, and M. Zolotarev, *Science* **287**, 2237 (2000).

<sup>2</sup>S. Khan, K. Holldack, T. Kachel, R. Mitzner, and T. Quast, *Phys. Rev. Lett.* **97**, 74801 (2006).

<sup>3</sup>P. Beaud, S. Johnson, A. Streun, R. Abela, D. Abramsohn, D. Grolimund, F. Krasniqi, T. Schmidt, V. Schlott, and G. Ingold, *Phys. Rev. Lett.* **99**, 174801 (2007).

<sup>4</sup>B. McNeil, *Nat. Photonics* **3**, 375 (2009).

<sup>5</sup>M. Abo-Bakr, J. Feikes, K. Holldack, P. Kuske, W. B. Peatman, U. Schade, G. Wüstefeld, and H.-W. Hübers, *Phys. Rev. Lett.* **90**, 094801 (2003).

<sup>6</sup>I. Radu, C. Stamm, N. Pontius, T. Kachel, P. Ramm, J.-U. Thiele, H. A. Dürr, and C. H. Back, *Phys. Rev. B* **81**, 104415 (2010).

<sup>7</sup>F. Zamponi, Z. Ansari, C. von Korff Schmising, P. Rothhardt, N. Zhavoronkov, M. Woerner, T. Elsaesser, M. Bargheer, T. Trobitzsch-Ryll, and M. Haschke, *Appl. Phys. A* **96**, 51 (2009).

- <sup>8</sup>J. Larsson, P. Heimann, A. Lindenberg, P. Schuck, P. Bucksbaum, R. Lee, H. Padmore, J. Wark, and R. Falcone, *App. Phys. A* **66**, 587 (1998).
- <sup>9</sup>M. Herzog, W. Leitenberger, R. Shayduk, R. M. van der Veen, C. J. Milne, S. L. Johnson, I. Vrejoiu, M. Alexe, D. Hesse, and M. Bargheer, *Appl. Phys. Lett.* **96**, 161906 (2010).
- <sup>10</sup>I. Vrejoiu, G. Le Rhun, L. Pintilie, D. Hesse, M. Alexe, and U. Gösele, *Adv. Mater.* **18**, 1657 (2006).
- <sup>11</sup>In this letter we adopt the notation of SL peak orders described in, e.g., G. Bauer and W. Richter, *Optical Characterization of Epitaxial Semiconductor Layers* (Springer, Berlin, 1996). The SRO/STO (002) ZOP corresponds to the (0 0 116) SL reflection of previous publications.
- <sup>12</sup>C. v. Korff Schmising, M. Bargheer, M. Kiel, N. Zhavoronkov, M. Woerner, T. Elsaesser, I. Vrejoiu, D. Hesse, and M. Alexe, *Phys. Rev. Lett.* **98**, 257601 (2007).
- <sup>13</sup>S. Yamanaka, T. Maekawa, H. Muta, T. Matsuda, S. Kobayashi, and K. Kurosaki, *J. Solid State Chem.* **177**, 3484 (2004).
- <sup>14</sup>Y. H. Ren, M. Trigo, R. Merlin, V. Adyam, and Q. Li, *Appl. Phys. Lett.* **90**, 251918 (2007).